Chinese Journal of
POLYMER SCIENCE

RESEARCH ARTICLE

https://doi.org/10.1007/s10118-022-2730-4
Chinese J. Polym. Sci. **2022**, *40*, 921–927

A Low Reorganization Energy and Two-dimensional Acceptor with Four End Units for Organic Solar Cells with Low E_{loss}

Hongbin Chen[a], Xiangjian Cao[a], Xiaoyun Xu[b], Chenxi Li[a], Xiangjian Wan[a], Zhaoyang Yao[a], and Yongsheng Chen[a*]

[a] *State Key Laboratory and Institute of Elemento-Organic Chemistry, The Centre of Nanoscale Science and Technology and Key Laboratory of Functional Polymer Materials, Renewable Energy Conversion and Storage Center (RECAST), College of Chemistry, Nankai University, Tianjin 300071, China*
[b] *State Key Laboratory for Modification of Chemical Fibers and Polymer Materials, Center for Advanced Low-dimension Materials, College of Materials Science and Engineering, Donghua University, Shanghai 201620, China*

Electronic Supplementary Information

Abstract A novel two-dimensional A-D-A acceptor named as **CH8** with four electron-withdrawing end units has been successfully designed and synthesized. The enlarged conjugation in two directions renders **CH8** exhibit an extremely low electron reorganization energy of 98 meV, which makes **CH8** a potential candidate for outstanding organic semiconductor material. When blended with **PM6**, a considerate power conversion efficiency of 9.37% along with a high open-circuit voltage (V_{oc}) 0.889 V and low energy loss (E_{loss}) below 0.6 eV is achieved. These results indicate that the two-dimensional A-D-A molecule with four electron-withdrawing end units is an effective molecular design strategy to achieve lower voltage loss and also possible high performance for organic photovoltaics if ideal morphology could be achieved.

Keywords Two-dimensional A-D-A acceptor; Reorganization energy; Energy loss (E_{loss}); Organic photovoltaics

Citation: Chen, H.; Cao, X.; Xu, X.; Li, C.; Wan, X.; Yao, Z.; Chen, Y. A low reorganization energy and two-dimensional acceptor with four end units for organic solar cells with low E_{loss}. *Chinese J. Polym. Sci.* **2022**, *40*, 921–927.

INTRODUCTION

Bulk heterojunction (BHJ) organic solar cells (OSCs) have attracted widespread interest in the renewable energy community due to their lightweight, flexibility, tunable transparency and color, and low-cost fabrication techniques.[1–4] The photoactive materials in OSCs are composed of electron donors and electron acceptors. Currently, non-fullerene acceptors (NFAs) play a crucial role in OSCs and have attracted extensive attention due to their high performance and tunable energy levels.[5,6] Among them, the main focus is on the linear-shaped one-dimensional NFAs with an acceptor-donor-acceptor (A-D-A) architecture[7] like **ITIC**,[8,9] **F** series,[10,11] **Y6** and their derivatives *etc*.,[12,13] which has been the main driving force for the current over 19% power conversion efficiencies (PCEs).[14]

Currently, the widely explored NFAs are most with one direction conjugation along the main backbone in such as linear-shaped one-dimensional NFAs mentioned above. It is believed that there would be many potential advantages in electron reorganization energy, molecular packing, charge transport and light harvesting if the conjugation could be extended into two dimensions such as in two-dimensional (2D) acceptors.[15,16] Recently, two-dimensional (2D) star-shaped fused-ring electron acceptors with three electron-withdrawing end units have been reported with improved photoelectric parameters and ~10% PCE.[16–18] However, very few investigations have been carried out for 2D NFAs with other architectures, which might have limited the potentially high performance of the largely available 2D NFAs with various architectures. Thus, it would be interesting and desired to study such 2D NFAs with different architectures in terms of both potentially high performance and understanding of the relationship between structure and properties.

In this work, we designed and synthesized **CH8**, a 2D acceptor with four electron-withdrawing end units with conjugation extended into two perpendicular directions (Fig. 1a). **CH8** has an extremely low electron reorganization energy by the density functional theory (DFT) calculations, with an intense absorption in the region of 300–850 nm and appropriate energy levels as an electron acceptor for OSCs. When blended with **PM6**,[19] a considerate PCE of 9.37% along with a high open-circuit voltage (V_{oc}) 0.889 V and low energy loss (E_{loss}) below 0.6 eV were achieved. And the blend film exhibited a good electron mobility of 1.52×10^{-4} $cm^2 \cdot V^{-1} \cdot s^{-1}$ and a favorable face-on stacking orientation morphology. The moderate performance is believed mainly due to the inferior morphology of the active layer because of rather poor phase se-

* Corresponding author, E-mail: yschen99@nankai.edu.cn
Special Issue: Organic Photovoltaic Polymers
Received February 3, 2022; Accepted March 7, 2022; Published online June 6, 2022

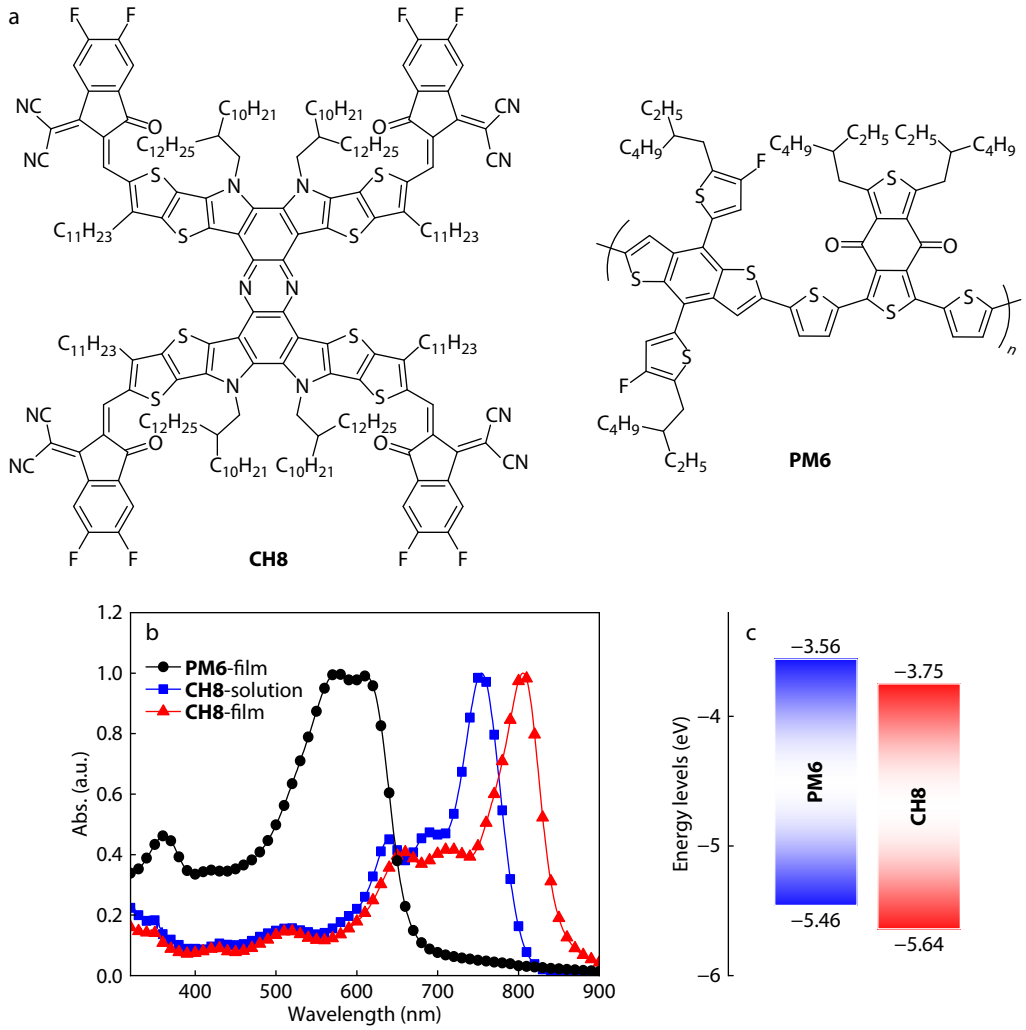

Fig. 1 (a) Molecular structures of **CH8** and **PM6**; (b) Normalized absorption spectra of **PM6** in films and **CH8** in solution and films, respectively; (c) Energy levels diagram of **CH8** and **PM6**.

paration of the D/A and thus no ideal nanoscale D/A penetrating network could form.

EXPERIMENTAL

The details of material characterizations and experimental methods are presented in the electronic supplementary information (ESI).

RESULTS AND DISCUSSION

Synthesis and Characterization

The overall synthesized route to **CH8** is displayed in Scheme 1 and the detailed procedures and characterizations are described in ESI. We successfully obtained 2D donor core (compound **2**) in a reasonable yield with the key step of phenazine conversion from benzothiadiazole. As shown in Scheme 1, this challenging conversion was achieved by an *in situ* condensation between two intermediates, **1a** and **1b**, which were generated from reduction and followed oxidation of commercially available compound **1**.[15] After formylation of the resulting compound **2** by Vilsmeier reagent, **CH8** was finally synthesized by Knoevenagel condensation reaction between compound **3** and the end unit **4**.

DFT calculations were conducted to evaluate the molecular conformations of **CH8**. The detailed calculated method was described in ESI. Through DFT calculations shown in Fig. S1 (in ESI), **CH8** has good planarity along the *y* axis, which could be favorable for intramolecular charge transfer (ICT)[20] and intermolecular *π*-*π* stacking. The formed a relatively larger dihedral angle of ~20° along the *x* axis between the two major molecular planes, together with long alkyl chains which might weaken self-aggregation of **CH8** to have small/weakened domain size in blend films for OSCs. The long alkyl chains on sp^2 N atoms of **CH8** are essential for favorable solubility which is the prerequisite for solution-processed solar cells. However, the increasing steric hindrance caused by the overlong alkyl chains could go against the closely *π*-*π* stacking between neighboring molecule pairs. This might lead to the inferior crystalline of **CH8** and unsatisfactory phase separation in blended film. In addition, **CH8** exhibits the clear A-D-A feature demonstrated by its characteristic peak-valley-peak plot along the *x* and *y* directions of molecular backbone for its frontier orbital charge density difference (ΔQ),[7] respectively (Fig. S2 in ESI). It has been proved that the

https://doi.org/10.1007/s10118-022-2730-4

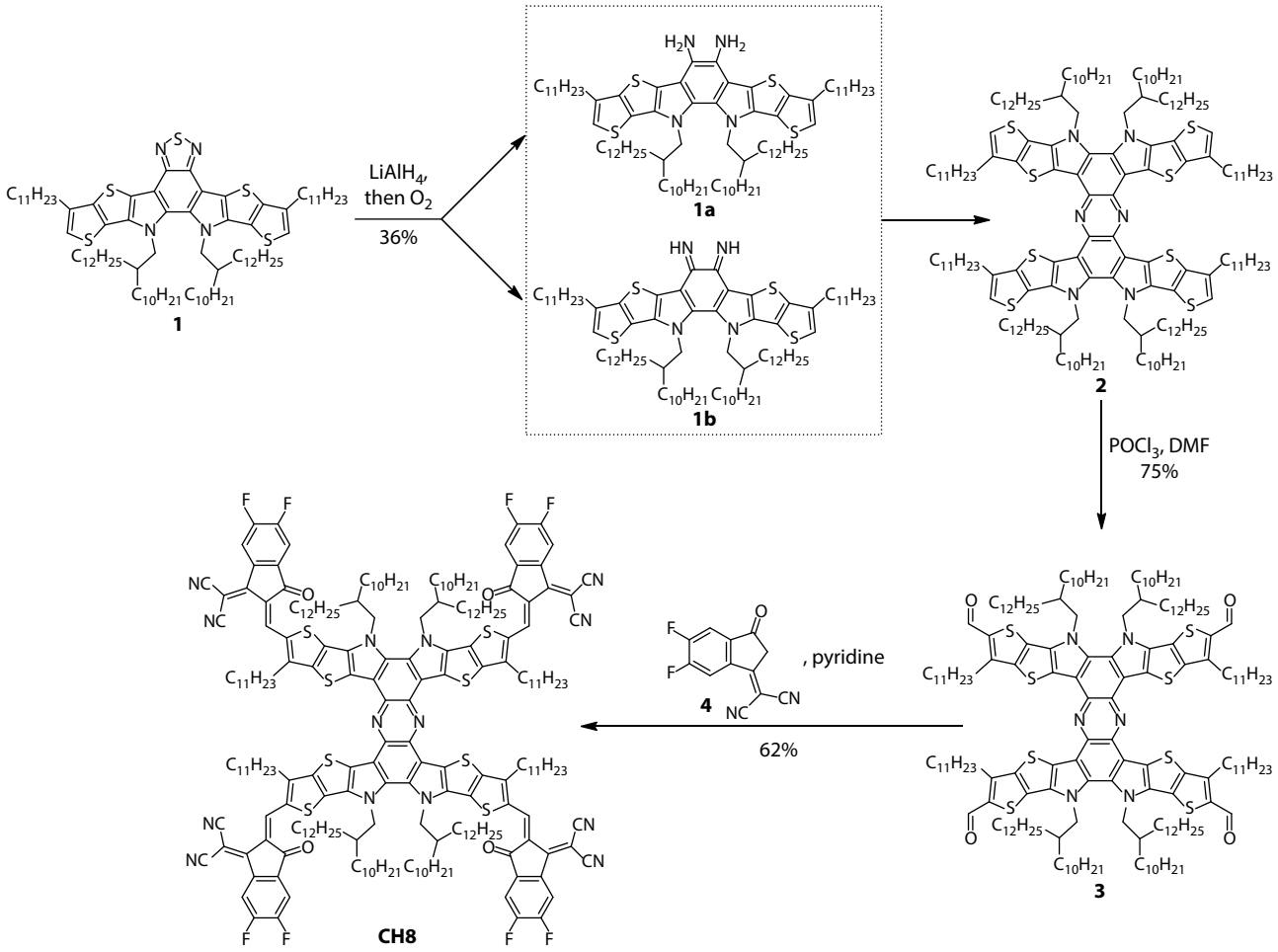

Scheme 1 The overall synthesis route to **CH8**.

A-D-A feature of molecule would endow enhanced exciton separation and charge transportation and thus facilitate OPV performance in blend films.[7] In addition, reorganization energy is related to the rate of charge transfer, which has been regarded as one of the critical parameters in the design of high-efficiency molecules for OSCs. A small reorganization energy of molecule is expected to give rise to a large carrier mobility in solid state and also could reduce the E_{loss} in solar cells. Therefore, the electron reorganization energy of **CH8** has been investigated in this work. Low electron reorganization energies (λ) values would be achieved when the neutral and charged species have very similar geometries, and excess charge can be effectively delocalized over the entire molecule.[21] We find that the enlarged conjugation 2D **CH8** indeed has a very low computed internal λ of 98 meV, and is lower even than those of **ITIC** and **Y6** analogues.[21,22] This is expected to be beneficial for high mobilities and improved charge transport, which is discussed below.[23] The detailed computational methods and a comparative Table S2 were shown in ESI.

Fig. 1(b) shows the normalized absorption spectra of **CH8** in solution and thin film, with a large molar absorption coefficient of 3.28×10^5 $M^{-1}\cdot cm^{-1}$ in chloroform solution. The maximum absorption peak of **CH8** has an obvious redshift with 52 nm from solution to film, which suggests that the 2D molecule possesses relatively strong intermolecular π-π interaction. The cyclic voltammetry was performed to evaluate the frontier orbital energy levels of **CH8** and the HOMO and LUMO energy levels were shown in Fig. 1(c) and Fig. S3 (in ESI). This higher LUMO energy level of **CH8** at −3.75 eV than that of state-of-the-art acceptor **Y6**[13] indicates that OSCs based **CH8** would have an improved V_{oc}. The energy levels derived from CVs are also in accordance with the results from theoretical calculations (Fig. S4 in ESI). The detailed parameters of physicochemical properties for **CH8** are summarized in Table S1 (in ESI).

Photovoltaic Performance and Charge Transport Measurements

All the OSC devices were fabricated by a conventional structure of ITO/PEDOT:PSS/active layer/PDINO/Ag to evaluate their photovoltaic performance and polymer **PM6**[19] was selected as the donor in active layer considering its matching energy levels and complementary absorption with **CH8**. The optimization of OSCs is summarized in Table S3 (in ESI) and the optimized photovoltaic parameters are shown in Table 1. The most optimal device conditions were prepared by mixing **PM6** and **CH8** in a 1:0.8 weight ratio into CF without additive and under thermal annealing at 80 °C for 5 min, resulting a PCE of 9.37% with a V_{oc} of 0.889 V, short current densities (J_{sc}) of 19.70 $mA\cdot cm^{-2}$ and fill factor (FF) of 53.5%.

https://doi.org/10.1007/s10118-022-2730-4

The optimal current density-voltage (*J-V*) curve of champion OSCs based on **CH8** was recorded in Fig. 2(a). As shown in Fig. 2(b), The **PM6**:**CH8**-based cell shows good photo response in the wavelength range of 300–850 nm, especially with a EQE value over 70% at 500–650 nm. The integrated current density is 19.31 mA·cm^{-2}, which is consistent the value obtained from the *J-V* measurement within a 2% error. Note, while the FF is quite low compared with most of the state-of-the-art materials, its PCE of 9.37% is still among the highest PCE in 2D acceptor based on OSCs,[16] indicating that 2D NFAs with four end units in two perpendicular directions are potential candidates for high effective OSCs. In addition, the **PM6**:**CH8** blend shows a hole and electron mobilities of 0.80×10^{-4} and 1.52×10^{-4} cm^2·V^{-1}·s^{-1} by space charge limited current method, (Table 1 and Fig. S5 in ESI) respectively. The outstanding charge transport ability is related to the very small reorganization energy calculated by DFT.

Note from above discussion, the hole and electron mobilities of active layer of **PM6**:**CH8** blend are high and also balanced and **CH8** also has a relatively large molar absorption coefficient and marching energy levels with the donor of **PM6**. Thus, the observed moderate PCE should mainly come from the possible unsatisfactory morphology in the active layer, clearly indicated by the low FF.

Morphology Analysis

To have an investigation of the correlation between the morphology and photovoltaic properties, grazing-incidence wide-angle X-ray scattering (GIWAXS) and atomic force microscopy (AFM) were applied to explore the stacking and the surface morphology of **CH8** in films. As shown in Figs. 3(a) and 3(b), (010) diffraction peak at q≈1.6 Å^{-1} in the out-of-plane (OOP) direction and (100) diffraction peak at q≈0.3 Å^{-1} in the in-plane (IP) direction were observed in **CH8** neat film, which is classified into a preferential face-on orientation.[12] And the favorable face-on orientation of packing, which is in favor of the efficient charge transport, is also kept in **CH8** blend films. Note from the 2D GIWAXS patterns of **CH8** neat film and **PM6**:**CH8** blend film shown in Figs. 3(a) and 3(b), there is very little clear crystalline pattern observed in the both neat **CH8** and its blend films with **PM6**. Especially, the OOP π-π diffraction peak at ≈1.6 Å^{-1} comes with a very small crystalline coherence length (CCL) of only 17 Å in **CH8** neat film and 7 Å in **PM6**:**CH8** blend film, which indicates that **CH8** molecules in films do not pack in a well-ordered pattern.[24] Note, the reduced CCL of **PM6**:**CH8** blend film from **CH8** neat film further indicates that **CH8** has even weakened crystallization tendency in the blend film. The clearest OOP peak at ≈0.36 Å^{-1}, which comes with a crystalline coherence length (CCL) of 112 Å for **CH8** neat film and 74 Å for **PM6**:**CH8** blend film, respectively, also shows the reduced crystallization tendency in the blend film. The largely weakened crystallization tendency from **CH8** neat film to **PM6**:**CH8** blend films indicates a good miscibility between **PM6** and **CH8**, which would lead to an unsatisfactory phase separation. As shown in Fig. 3(c) and Fig S6 (in ESI), the AFM images also clearly exhibited the weakened crystallization tendency from **CH8** neat film to **PM6**:**CH8** blend film and the unsatisfactory phase separation of the donor and acceptor could be observed in **PM6**:**CH8** blend film. The unsatisfactory phase separation and inferior crystalline of **CH8** might also related with long alkyl chains on sp^2 N atoms and its relatively larger dihedral angle shown in Fig. S1 (in ESI), which should probably account for the low FF of only 54%, and thus considerate PCE.[25]

Energy Loss Analysis

Energy loss (E_{loss}) is one of important parameters of limiting PCE of OSCs by influencing V_{oc}.[26] Therefore, the E_{loss} of **CH8**-based OSCs was studied according to the framework of Marcus theory.[27] In general, E_{loss} in OSCs can be regarded originating from three parts: ΔE_{CT}, ΔV_r and ΔV_{nr}.[28] Among them, ΔE_{CT} contributing to the first part of voltage loss is the energetic difference between the singlet excited state and charge transfer (CT) state. ΔV_r and ΔV_{nr} are the voltage loss terms related to the radiative and non-radiative decay rate of CT states,[29]

Table 1 Summary of device parameters of the optimized OSCs based on **CH8**. [a]

Active layer	V_{oc} (V)	J_{sc} (mA·cm^{-2})	Calcd. J_{sc} [b] (mA·cm^{-2})	FF (%)	PCE (%)	μ_e/μ_h [c] (10^{-4} cm^2·V^{-1}·s^{-1})
PM6:**CH8**	0.889(0.877±0.011)	19.70(19.12±0.35)	19.31	53.5(52.5±1.4)	9.37(8.81±0.25)	1.52/0.80

[a] Optimal and statistical results are listed outside of parentheses and in parentheses, respectively. [b] Current density calculated from EQE curve. [c] μ_e and μ_h are electron and hole mobilities of optimized **PM6**:**CH8** blends by SCLC measurements, respectively.

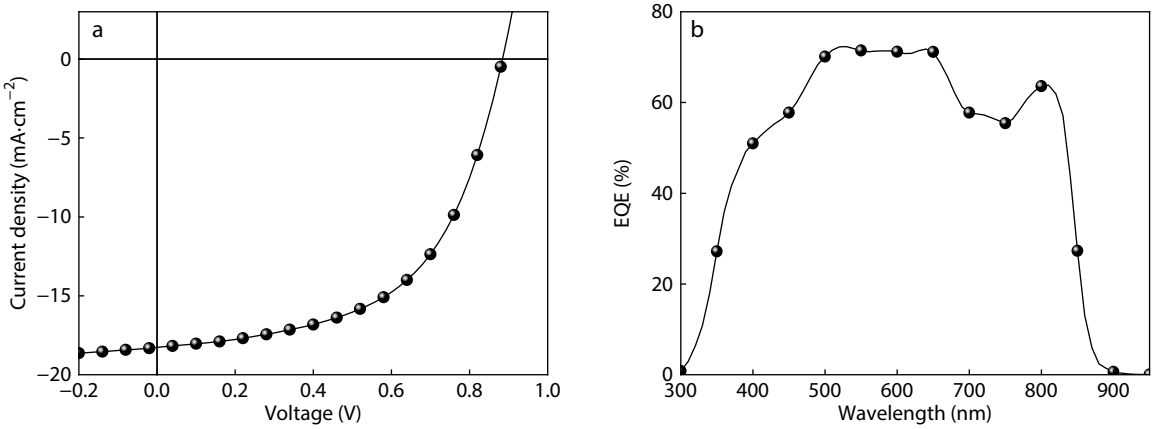

Fig. 2 (a) *J-V* curve and (b) EQE curve of the device based on optimized **PM6**:**CH8**.

https://doi.org/10.1007/s10118-022-2730-4

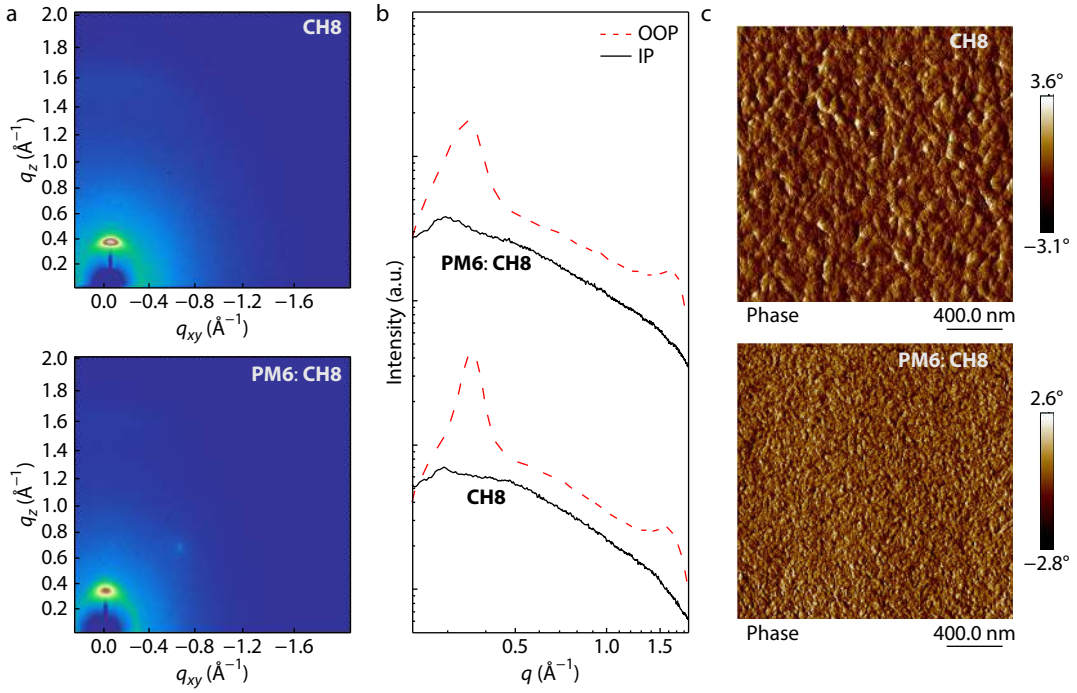

Fig. 3 (a) 2D GIWAXS patterns of **CH8** pure film and **PM6**:**CH8** blend film and (b) the corresponding IP (black solid line) and OOP (red dash line) extracted line-cut profiles; (c) AFM phase images of **CH8** pure film and **PM6**:**CH8** film.

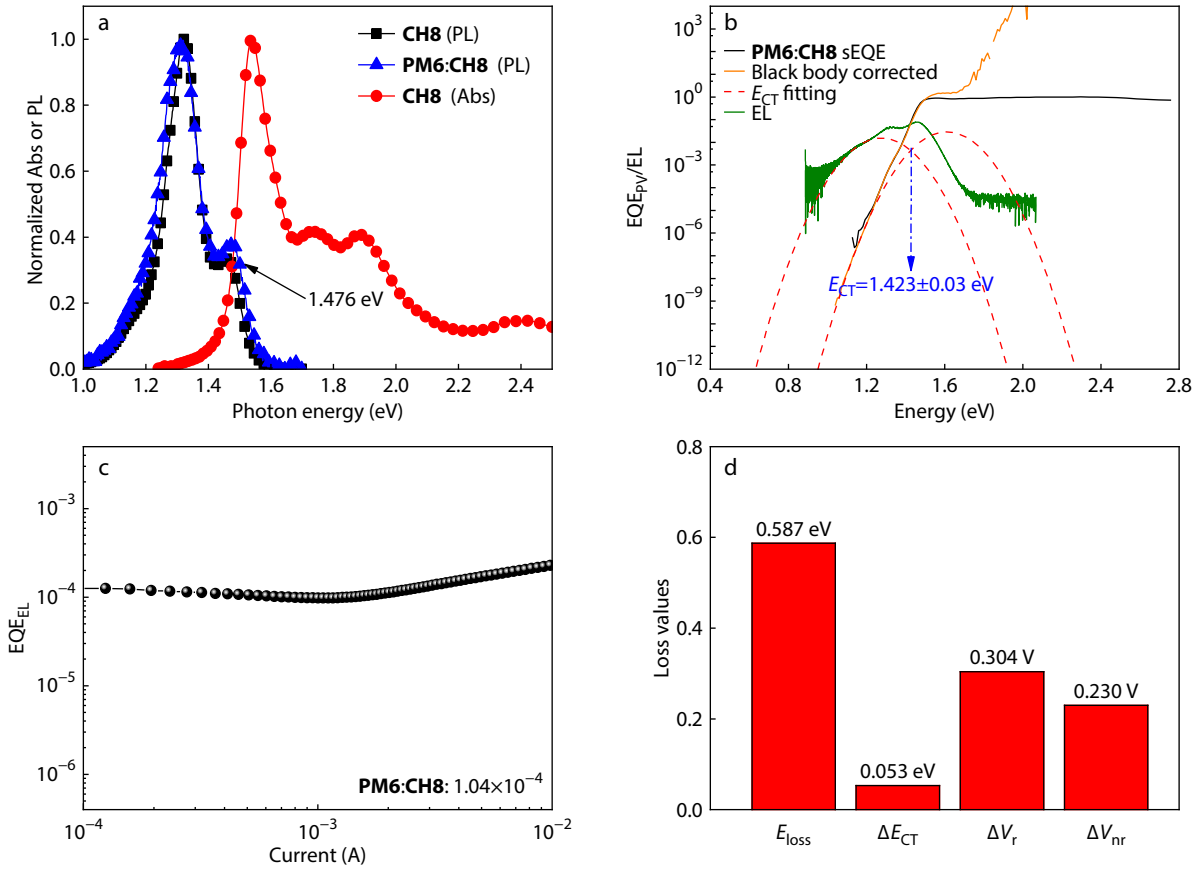

Fig. 4 (a) Details of optical E_g determination of **CH8**-based OSCs; (b) Sensitive external quantum efficiency (sEQE) spectra and electroluminescence (EL) spectra, and the fitting results for **CH8**-based device; (c) EQE$_{EL}$ spectra of the **CH8**-based OSC; (d) Detailed E_{loss}s of **CH8**-based device.

https://doi.org/10.1007/s10118-022-2730-4

respectively, and the suppression of non-radiative recombination is the most-concerned part to further improve the V_{oc} and PCEs of OSCs.[30]

As shown in Fig. 4(a), there is no obvious shift in the emission spectra onsets between the normalized photoluminescence (PL) spectra of the **CH8** blend and neat films. Therefore, the E_g of **CH8** was determined by the crossing point of emission and absorption spectra of its neat film.[31] Based on the equation: $E_{loss} = E_g - eV_{oc}$, the E_{loss} of **CH8**-based OSCs was obtained as 0.587 eV, which is smaller than those of **ITIC**[8] and **F**[11] series acceptors based OSCs and is comparative to that of state-of-the-art OSCs (0.5–0.6 eV).[12,26,32] The low E_{loss} should come from suppressed non-radiative recombination loss. Note the ΔE_{CT} determined by fitting the highly sensitive EQE (sEQE) of **CH8**-based solar cells is only 0.053 eV (Figs. 4b and 4d). Thus, the smaller energetic difference between the singlet excited CT states could enlarge the radiative rate of CT state *via* an intensity borrowing mechanism, leading to a small E_{loss}.[33] The small E_{loss} is also consistent with the observed high emission efficiency (EQE_{EL}) value of over 10^{-4} for **CH8**-based OSCs (Fig. 4c). With these, a rather small ΔV_{nr} of 0.230 V is obtained by the equation: $\Delta V_{nr} = -(kT/q)\ln(1/EQE_{EL})$.[34] The detailed data about E_{loss} of **CH8**-based OSCs are summarized in Fig. 4(d). These results indicate that 2D acceptor with four end units is potential molecular design strategy in suppressing E_{loss} and V_{nr}.

CONCLUSIONS

In summary, a novel two-dimensional A-D-A acceptor with four electron-withdrawing end units and conjugation extended into two perpendicular directions has been successfully designed and synthesized. Accompanied by its enlarged conjugation extension, **CH8** has an extremely low electron reorganization energy of 98 meV, which is consistent with its outstanding charge transport material. While a moderate PCE of 9.37% has been achieved, though still high among 2D acceptors, it gave a high V_{oc} of 0.889 V, and a quite small E_{loss} of 0.587 eV for its devices with **PM6** as the donor. The significantly reduced E_{loss} and ΔV_{nr} are believed to be due to the increased radiative recombination rate, partially contributed by its relatively high CT state. The main reason for the moderate PCE of its OSCs is believed due to the unsatisfied morphology of the active layer. Considering their advantage of smaller E_{loss} and higher V_{oc}, it is believed that these 2D conjugation molecules could have much higher performance if their morphology could be further tuned.

NOTES

The authors declare no competing financial interest.

Electronic Supplementary Information

Electronic supplementary information (ESI) is available free of charge in the online version of this article at http://doi.org/10.1007/s10118-022-2730-4.

ACKNOWLEDGMENTS

This work was financially supported by the National Natural Science Foundation of China (Nos. 21935007, 52025033 and 51873089) and Ministry of Science and Technology (No. 2019YFA0705900) of China, Tianjin city (No. 20JCZDJC00740) and 111 Project (No. B12015). We also acknowledge the GIWAXS measurements provided by Prof Zhixiang Wei at the National Center for Nanoscience and Technology, CAS, Beijing 100190, China. All the theoretical calculations were performed on National Supercomputer Center in Guangzhou.

REFERENCES

1 Chen, H.; Zhang, R.; Chen, X.; Zeng, G.; Kobera, L.; Abbrent, S.; Zhang, B.; Chen, W.; Xu, G.; Oh, J.; Kang, S. H.; Chen, S.; Yang, C.; Brus, J.; Hou, J.; Gao, F.; Li, Y.; Li, Y. A guest-assisted molecular-organization approach for >17% efficiency organic solar cells using environmentally friendly solvents. *Nat. Energy* **2021**, *6*, 1045–1053.

2 Hu, Z.; Wang, J.; Ma, X.; Gao, J.; Xu, C.; Yang, K.; Wang, Z.; Zhang, J.; Zhang, F. A critical review on semitransparent organic solar cells. *Nano Energy* **2020**, *78*, 105376.

3 Liu, S.; Chen, D.; Hu, X.; Xing, Z.; Wan, J.; Zhang, L.; Tan, L.; Zhou, W.; Chen, Y. Printable and large-area organic solar cells enabled by a ternary pseudo-planar heterojunction strategy. *Adv. Funct. Mater.* **2020**, *30*, 2003223.

4 Song, W.; Liu, Y.; Fanady, B.; Han, Y.; Xie, L.; Chen, Z.; Yu, K.; Peng, X.; Zhang, X.; Ge, Z. Ultra-flexible light-permeable organic solar cells for the herbal photosynthetic growth. *Nano Energy* **2021**, *86*, 106044.

5 Chai, G.; Chang, Y.; Zhang, J.; Xu, X.; Yu, L.; Zou, X.; Li, X.; Chen, Y.; Luo, S.; Liu, B.; Bai, F.; Luo, Z.; Yu, H.; Liang, J.; Liu, T.; Wong, K. S.; Zhou, H.; Peng, Q.; Yan, H. Fine-tuning of side-chain orientations on nonfullerene acceptors enables organic solar cells with 17. 7% efficiency. *Energy Environ. Sci.* **2021**, *14*, 3469–3479.

6 Li, W.; Liu, D.; Wang, T. Stability of non-fullerene electron acceptors and their photovoltaic devices. *Adv. Funct. Mater.* **2021**, *31*, 2104552.

7 Wan, X.; Li, C.; Zhang, M.; Chen, Y. Acceptor–donor–acceptor type molecules for high performance organic photovoltaics—chemistry and mechanism. *Chem. Soc. Rev.* **2020**, *49*, 2828–2842.

8 Lin, Y.; Wang, J.; Zhang, Z. G.; Bai, H.; Li, Y.; Zhu, D.; Zhan, X. An electron acceptor challenging fullerenes for efficient polymer solar cells. *Adv. Mater.* **2015**, *27*, 1170–1174.

9 Yao, H.; Cui, Y.; Yu, R.; Gao, B.; Zhang, H.; Hou, J. Design, synthesis, and photovoltaic characterization of a small molecular acceptor with an ultra-narrow band gap. *Angew. Chem. Int. Ed.* **2017**, *56*, 3045–3049.

10 Ke, X.; Meng, L.; Wan, X.; Li, M.; Sun, Y.; Guo, Z.; Wu, S.; Zhang, H.; Li, C.; Chen, Y. The rational and effective design of nonfullerene acceptors guided by a semi-empirical model for an organic solar cell with an efficiency over 15%. *J. Mater. Chem. A* **2020**, *8*, 9726–9732.

11 Qiu, N.; Zhang, H.; Wan, X.; Li, C.; Ke, X.; Feng, H.; Kan, B.; Zhang, H.; Zhang, Q.; Lu, Y.; Chen, Y. A new nonfullerene electron acceptor with a ladder type backbone for high-performance organic solar cells. *Adv. Mater.* **2017**, *29*, 1604964.

12 Li, C.; Zhou, J.; Song, J.; Xu, J.; Zhang, H.; Zhang, X.; Guo, J.; Zhu, L.; Wei, D.; Han, G.; Min, J.; Zhang, Y.; Xie, Z.; Yi, Y.; Yan, H.; Gao, F.; Liu, F.; Sun, Y. Non-fullerene acceptors with branched side chains and improved molecular packing to exceed 18% efficiency in organic solar cells. *Nat. Energy* **2021**, *6*, 605–613.

13 Yuan, J.; Zhang, Y.; Zhou, L.; Zhang, G.; Yip, H. L.; Lau, T. K.; Lu, X.; Zhu, C.; Peng, H.; Johnson, P. A.; Leclerc, M.; Cao, Y.; Ulanski, J.; Li, Y.; Zou, Y. Single-junction organic solar cell with over 15%

efficiency using fused-ring acceptor with electron-deficient core. *Joule* **2019**, *3*, 1140–1151.
14 Cui, Y.; Xu, Y.; Yao, H.; Bi, P.; Hong, L.; Zhang, J.; Zu, Y.; Zhang, T.; Qin, J.; Ren, J.; Chen, Z.; He, C.; Hao, X.; Wei, Z.; Hou, J. Single-junction organic photovoltaic cell with 19% efficiency. *Adv. Mater.* **2021**, *33*, 2102420.
15 Chen, H.; Zou, Y.; Liang, H.; He, T.; Xu, X.; Zhang, Y.; Ma, Z.; Wang, J.; Zhang, M.; Li, Q.; Li, C.; Long, G.; Wan, X.; Yao, Z.; Chen, Y. Lowing the energy loss of organic solar cells by molecular packing engineering *via* multiple molecular conjugation extension. *Sci. China Chem.* **2022**, *65*, https://doi.org/10.1007/s11426-022-1264-y.
16 Cai, G.; Wang, W.; Zhou, J.; Xiao, Y.; Liu, K.; Xie, Z.; Lu, X.; Lian, J.; Zeng, P.; Wang, Y.; Zhan, X. Comparison of linear- and star-shaped fused-ring electron acceptors. *ACS Mater. Lett.* **2019**, *1*, 367–374.
17 Li, S.; Liu, W.; Shi, M.; Mai, J.; Lau, T.-K.; Wan, J.; Lu, X.; Li, C. Z.; Chen, H. A spirobifluorene and diketopyrrolopyrrole moieties based non-fullerene acceptor for efficient and thermally stable polymer solar cells with high open-circuit voltage. *Energy Environ. Sci.* **2016**, *9*, 604–610.
18 Liu, D.; Wang, T.; Chang, Z.; Zheng, N.; Xie, Z.; Liu, Y. Fused or unfused? Two-dimensional non-fullerene acceptors for efficient organic solar cells *J. Mater. Chem. A* **2021**, *9*, 2319–2324.
19 Qian, D.; Ye, L.; Zhang, M.; Liang, Y.; Li, L.; Huang, Y.; Guo, X.; Zhang, S.; Tan, Z. A.; Hou, J. Design, application, and morphology study of a new photovoltaic polymer with strong aggregation in solution state. *Macromolecules* **2012**, *45*, 9611–9617.
20 Li, S.; Zhang, Y.; Mei, S.; Kong, X.; Yang, M.; Hu, Z.; Wu, W.; He, J.; Tan, H. A molecular engineering strategy of phenylamine-based zinc-porphyrin dyes for dye-sensitized solar cells: synthesis, characteristics, and structure-performance relationships. *ACS Appl. Energy Mater.* **2021**, *4*, 9267–9275.
21 Swick, S. M.; Zhu, W.; Matta, M.; Aldrich, T. J.; Harbuzaru, A.; Lopez Navarrete, J. T.; Ponce Ortiz, R.; Kohlstedt, K. L.; Schatz, G. C.; Facchetti, A.; Melkonyan, F. S.; Marks, T. J. Closely packed, low reorganization energy π-extended postfullerene acceptors for efficient polymer solar cells. *Proc. Natl. Acad. Sci. U.S.A.* **2018**, *115*, E8341.
22 Li, G.; Zhang, X.; Jones, L. O.; Alzola, J. M.; Mukherjee, S.; Feng, L. W.; Zhu, W.; Stern, C. L.; Huang, W.; Yu, J.; Sangwan, V. K.; DeLongchamp, D. M.; Kohlstedt, K. L.; Wasielewski, M. R.; Hersam, M. C.; Schatz, G. C.; Facchetti, A.; Marks, T. J. Systematic merging of nonfullerene acceptor π-extension and tetrafluorination strategies affords polymer solar cells with >16% efficiency. *J. Am. Chem. Soc.* **2021**, *143*, 6123–6139.
23 Stehr, V.; Fink, R. F.; Tafipolski, M.; Deibel, C.; Engels, B. Comparison of different rate constant expressions for the prediction of charge and energy transport in oligoacenes. *WIREs Comput. Mol. Sci.* **2016**, *6*, 694–720.
24 Zhang, G.; Chen, X. K.; Xiao, J.; Chow, P. C. Y.; Ren, M.; Kupgan, G.; Jiao, X.; Chan, C. C. S.; Du, X.; Xia, R.; Chen, Z.; Yuan, J.; Zhang, Y.; Zhang, S.; Liu, Y.; Zou, Y.; Yan, H.; Wong, K. S.; Coropceanu, V.; Li, N.; Brabec, C. J.; Bredas, J. L.; Yip, H. L.; Cao, Y. Delocalization of exciton and electron wavefunction in non-fullerene acceptor molecules enables efficient organic solar cells. *Nat. Commun.* **2020**, *11*, 3943.
25 Liu, Q.; Jiang, Y.; Jin, K.; Qin, J.; Xu, J.; Li, W.; Xiong, J.; Liu, J.; Xiao, Z.; Sun, K.; Yang, S.; Zhang, X.; Ding, L. 18% Efficiency organic solar cells. *Sci. Bull.* **2020**, *65*, 272–275.
26 Liu, S.; Yuan, J.; Deng, W.; Luo, M.; Xie, Y.; Liang, Q.; Zou, Y.; He, Z.; Wu, H.; Cao, Y. High-efficiency organic solar cells with low non-radiative recombination loss and low energetic disorder. *Nat. Photon.* **2020**, *14*, 300–305.
27 Marcus, R. A. Relation between charge transfer absorption and fluorescence spectra and the inverted region. *J. Phys. Chem. C* **1989**, *93*, 3078–3086.
28 Liu, H.; Li, M.; Wu, H.; Wang, J.; Ma, Z.; Tang, Z. Improving quantum efficiency in organic solar cells with a small energetic driving force. *J. Mater. Chem. A* **2021**, *9*, 19770–19777.
29 Eisner, F. D.; Azzouzi, M.; Fei, Z.; Hou, X.; Anthopoulos, T. D.; Dennis, T. J. S.; Heeney, M.; Nelson, J. Hybridization of local exciton and charge-transfer states reduces nonradiative voltage losses in organic solar cells. *J. Am. Chem. Soc.* **2019**, *141*, 6362–6374.
30 Gillett, A. J.; Privitera, A.; Dilmurat, R.; Karki, A.; Qian, D.; Pershin, A.; Londi, G.; Myers, W. K.; Lee, J.; Yuan, J.; Ko, S. J.; Riede, M. K.; Gao, F.; Bazan, G. C.; Rao, A.; Nguyen, T. Q.; Beljonne, D.; Friend, R. H. The role of charge recombination to triplet excitons in organic solar cells. *Nature* **2021**, *597*, 666–671.
31 Wang, Y.; Qian, D.; Cui, Y.; Zhang, H.; Hou, J.; Vandewal, K.; Kirchartz, T.; Gao, F. Optical gaps of organic solar cells as a reference for comparing voltage losses. *Adv. Energy Mater.* **2018**, *8*, 1801352.
32 Chen, X.-K.; Qian, D.; Wang, Y.; Kirchartz, T.; Tress, W.; Yao, H.; Yuan, J.; Hülsbeck, M.; Zhang, M.; Zou, Y.; Sun, Y.; Li, Y.; Hou, J.; Inganäs, O.; Coropceanu, V.; Bredas, J. L.; Gao, F. A unified description of non-radiative voltage losses in organic solar cells. *Nat. Energy* **2021**, *6*, 799–806.
33 Qian, D.; Zheng, Z.; Yao, H.; Tress, W.; Hopper, T. R.; Chen, S.; Li, S.; Liu, J.; Chen, S.; Zhang, J.; Liu, X. K.; Gao, B.; Ouyang, L.; Jin, Y.; Pozina, G.; Buyanova, I. A.; Chen, W. M.; Inganäs, O.; Coropceanu, V.; Bredas, J. L.; Yan, H.; Hou, J.; Zhang, F.; Bakulin, A. A.; Gao, F. Design rules for minimizing voltage losses in high-efficiency organic solar cells. *Nat. Mater.* **2018**, *17*, 703–709.
34 Englman, R.; Jortner, J. The energy gap law for radiationless transitions in large molecules. *Molec. Phys.* **1970**, *18*, 145–164.